

# Corrosion Enhancement of PM Processed Magnesium by Turning Native Oxide on Mg Powders into Carbonates

Veronika Nagy Trembošová\*, Štefan Nagy, Martin Nosko, Peter Švec, Matej Štěpánek, Otto Bajana

**Abstract:** In addition to its use as a lightweight material, pure magnesium is a promising candidate for prospective bioimplants considering its excellent biocompatible properties. Regardless of what Mg application is used, the ultimate goal is to improve magnesium's mechanical properties and degradation behaviour. Because of the high affinity for oxygen native oxide layer of gas-atomized powders is naturally formed in contact with the atmosphere. S/TEM investigation of the native oxide of the Mg powder particles revealed a nonhomogeneous nano-crystalline MgO layer. MgO is relatively soluble in water and does not provide sufficient corrosion protection. Among various surface treatment methods, conversion of the non-protective magnesium oxide to carbonate products is possible depending on the environmental conditions. This work used a simple experimental method using CO<sub>2</sub> and water vapour to achieve surface carbonation of Mg powders. Two carbonated samples and pure magnesium were prepared by direct extrusion. The samples after carbonation retained good mechanical properties and the layer of carbonates had a significant impact on corrosion resistance. 1 day carbonation resulted in transformation of native oxide into amorphous layer and reduction of corrosion rate. Longer carbonation (10 days) revealed layer growth and transformation of native oxide to crystalline nesquehonite structure.

**Keywords:** corrosion; magnesium powder; native oxide; surface modifications

## 1 INTRODUCTION

In recent years, an intensive effort was made to solve the main problems which limited the application of magnesium. Magnesium has become recognized as a structural material, which delivers, on the one hand, the essential advantages of reduced mass while retaining the suitable mechanical, thermal, and biodegradable properties that make it a desired candidate for advanced engineering in the aerospace industry, electronic devices or implant applications [1-3]. Still, on the other hand, pure magnesium's high susceptibility to corrosion holds it from fulfilling all possibilities.

Magnesium is a reactive metal, and under humid conditions, its corrosion resistance is strongly influenced by its high affinity for oxygen [4, 5]. Consequently, oxygen uptake from the surrounding atmosphere leads to the formation of a thermodynamically stable native MgO-layer with a thickness of 3 - 5 nm on the surface of the magnesium particles. In humid air, hydration of naturally grown magnesium oxide (MgO), uniformly adhering to the Mg surface, results in hydroxide (Mg(OH)<sub>2</sub>) formation [6, 7]. Several studies characterized the oxidation of magnesium and the surface structures, including usually a dense upper layer of Mg(OH)<sub>2</sub> on top of a porous layer of MgO on the Mg core [8-10].

Understanding and improving the corrosion behaviour of magnesium is vital for increasing its potential application. While the possibilities of enhancing the corrosion resistance by alloying are limited, a number of modification and coating methods have been developed [11, 12]. Surface modifications, among which the most frequently used, are chemical conversion coating [13], organic coating [14], and micro-arc oxidation coating [15] are an efficient way to isolate the metal core of magnesium from external environments.

Carbonate coatings fabricated by reacting with excited CO<sub>2</sub> or combining processing and heat-treatment of Mg-

based materials are promising methods for enhanced corrosion stability [16, 17]. MgCO<sub>3</sub> coating can be an effective barrier because it is sparingly soluble in water. However, the high thermodynamic equilibrium and the kinetics of the reaction at atmospheric pressure are very slow and require an extra excitation, such as heating to at least 400 °C [18, 19] or high energy electron beam [16]. Many different ways of preparing MgCO<sub>3</sub> are described in the literature. Recently most studies have focused on the reaction between CO<sub>2</sub> and metal oxides at low-temperature levels. Moreover, if water and CO<sub>2</sub> co-exist in the environment, MgCO<sub>3</sub> can be produced at atmospheric pressure [20].

Great effort has also been put into enhancing the strength of magnesium-based materials. Among various methods, powder metallurgy (PM) processing, in combination with severe plastic deformation (SPD) techniques, can be used to improve the microstructural and mechanical properties of magnesium. Compared with the casting process, the powder metallurgy (PM) route can positively affect the hardness, tensile and yield strength, and the development of a crystallographic texture [12, 21].

## 2 MATERIALS AND METHODS

The experiments were performed on pure Mg (99.98 %) atomized powder (IMR Metalle, Austria) with a size fraction value of 20 - 40 μm. Particle size distribution (PSD) was determined by a laser diffraction system (Fritsch Analysette 22 MicroTec device) with d<sub>50</sub> powder particle size values of 30 μm. The microstructure of the powders was studied by scanning electron microscopy (SEM, JEOL JSM-7600F) equipped with EDS, WDS, and EBSD detectors. The analysis was focused on the surface morphology and the microstructure of the samples after forward extrusion processing. The detailed microstructure of the native MgO and the extruded samples was examined using transmission electron microscopy (TEM, JEOL 1200FX) operated at 80

kV and a probe-corrected FEI/ThermoFisher Scientific Titan Themis 300 transmission electron microscope in scanning mode (STEM) at a 200 kV accelerating voltage. Direct observation of the native MgO surface layer on initial Mg powders was done using support Cu grids with lacey carbon film. For a more detailed characterization of the interface, standard preparation of bulk material was done using grinding, polishing, and final ion polishing (GatanPIPS-Cryo holder).

Diffraction data to confirm the layer transformation were measured on a Bruker D8 diffractometer with Co K  $\alpha$ max radiation (0,179 nm) in a parallel beam configuration. The measurement was performed at a constant angle of incidence of 10 degrees.

Carbonation of the Mg powder's surface was performed in a crucible placed over a Petri dish filled with distilled water in a closed desiccator under a CO<sub>2</sub> atmosphere for 1 and 10 days.

The powders were compacted by cold isostatic pressing (CIP) at a pressure of 300 MPa, with a short pressure endurance followed by slow decompression. The forward extrusion was performed on a custom-made laboratory hydraulic press at an average extrusion speed of 0,2 mm/s with a reduction ratio of 16:1. The extrudates were heated to 375 °C before extrusion for 15 minutes.

The mechanical testing was performed using tensile specimens with a gauge diameter of 3 mm and a length of 21 mm, which were machined in parallel to the direction of extrusion. The tensile tests were performed at 23 °C (RT) using a Zwick Roell 1474 machine in accordance with the ASTM E8 standard.

Immersion tests in Hanks' Balanced Salt Solution (HBSS) were performed to investigate the corrosion behaviour of the composites. An excess of HBSS was used to minimize the effect of the corrosion products on the kinetics of the reaction. Degradation of the samples along the immersion time was observed by monitoring the hydrogen evolution, then converted to corrosion rate according to the Eq. (1), where  $A$  denotes the reaction surface of the sample and  $t$  is the immersion time in HBSS. Each sample was immersed separately in HBSS for 48 hours at 37 °C. For corrosion tests, the non-treated sample was used as a reference, and it was compared to the sample carbonated for 24 hours.

$$CR = \frac{m_{Mg}}{A \cdot t} \quad (1)$$

### 3 RESULTS AND DISCUSSION

#### 3.1 Transformation of the Native Surface Oxide into Carbonates

To interpret the changes during a reaction of carbon dioxide with native MgO on the surface layer of Mg powders, we investigated the native oxide of the available atomized Mg powder. The particle morphology and size represent Fig. 1a, where the inhomogeneity of surface oxide is also visible. Further, TEM micrograph in Fig. 1b shows the cross-section

of Mg powder embedded in epoxy to investigate the native oxide layer. HAADF STEM micrograph at higher magnification in Fig. 1c shows the interface of the Mg core and native oxide layers. It's worth mentioning that the oxide layer consists of 2 layers: an inner dense layer (DL) and an outer porous layer (PL). FFT diffraction pattern taken from the porous layer area shows ring patterns that correspond with MgO cubic structure (Ref. num.: 00-004-0829). This indicates that the oxide layer consists of nanocrystals with different orientations. The micrograph also shows the porous character of the layer where the dark areas are pores. Atomic resolution micrograph taken from the dense layer proves that the primary oxide layer is also crystalline build-up from nanocrystals about 6 nm in size.

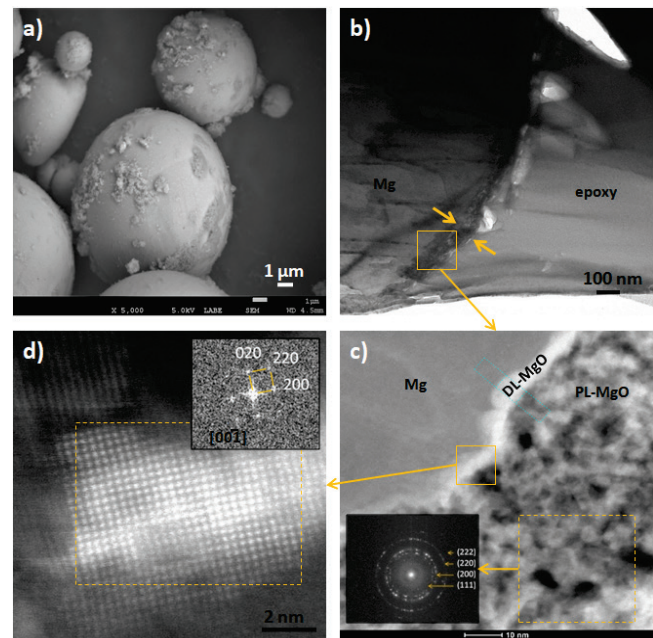


**Figure 1** SEM, TEM and STEM investigation of the native oxide on Mg powder: a) SEM micrograph of Mg powders; b) TEM micrograph of Mg powder embedded in epoxy; c) HAADF STEM image of the Mg/native oxide interface showing dense layer and porous layer with FFT diffraction from the porous oxide layer area; d) DF HRSTEM image of nanosized oxide from the dense layer with MgO crystal orientation [0 0-1]

SEM images of the Mg powder surface in Fig. 2a-c showed the morphology changes on the surface of Mg powder in the carbonation process after 1 day and 10 days. During the first day, the surface regions of the initially porous native oxide have changed to zones of amorphous hydrated magnesium carbonates without any visible evidence of the crystalline magnesium carbonate formation (Fig. 1b). Several crystalline carbonates can be recognized on the powder surface after 10 days (Fig. 1c). It can be seen changes in the form of plates uniformly adhering to the surface of powders. Adequately further investigation of the carbonation process was possible with direct TEM surface observations of carbonated powders. The native oxide layer in Fig. 2d is evident on the Mg powder without carbonation with MgO nanocrystalline porous layer, as mentioned before. After 1 day of carbonation, the porous oxide layer transforms to a denser layer, and the diffuse diffraction pattern indicates an

amorph transformation of the nanocrystalline MgO according to the CO<sub>2</sub> reaction. After 10 days of carbonation, we confirmed with SAEDP on the outer layer crystalline monoclinic nesquehonite phase (Ref. num.: 01-070-1433).

XRD measurement was performed on the Mg surface during carbonation, and the result is presented in Fig. 5. During the first days, the lack of carbonate peaks on the XRD pattern is likely the result of the formation of amorphous carbonate phases. The prolongation of the ageing period in the presence of a CO<sub>2</sub> environment is associated with the presence of hydrated carbonate phases, among which are dominant nesquehonite and hydromagnesite. After 10 days, nesquehonite is the dominant product of the reaction.

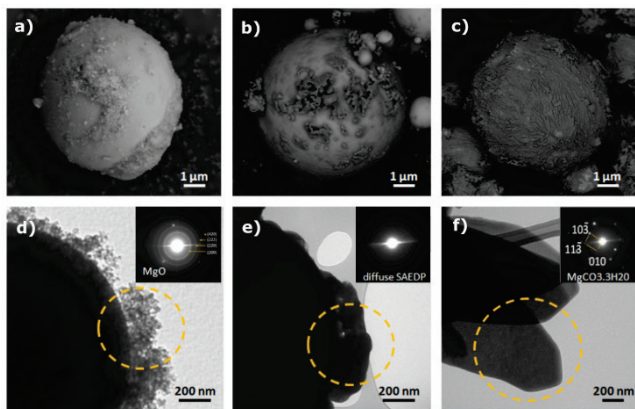


**Figure 2** The carbonation process investigated with SEM and TEM: changes on the powder's surface during the carbonation (a - c); direct observation of the powder native oxide layer with SAEDP analysis (d - f)

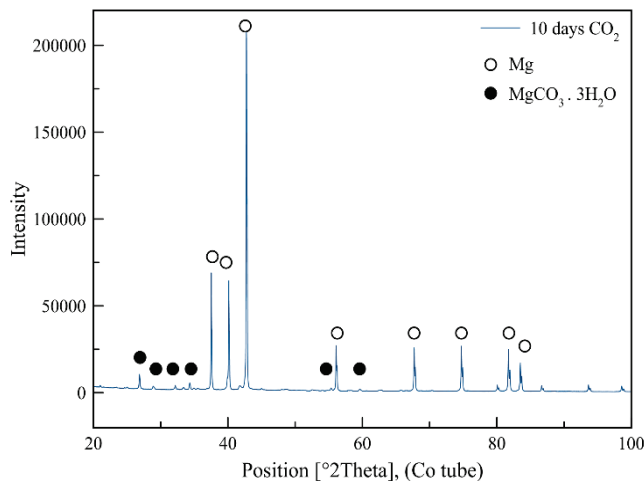


**Figure 3** XRD of the Mg powder after 10 days carbonation

### 3.2 Mechanical and Corrosion Properties of Extruded Samples

After carbonation, the powders were pressed and forward extruded into rods and then tested for mechanical and corrosion properties. Microstructure and EDS analysis after extrusion represent Fig. 4. The formed texture is evident according to the extended oxides supporting the oxygen map's EDS chemical analysis. The extruded material shows the nonhomogenous thickness of the deformed oxide or

carbonate layer. The carbon element map for short 1 day carbonation shows weakly the carbon element positions. However, after 10 days of carbonation, the carbon is strongly evident in the interface areas. Further analysis of the interface areas was investigated by TEM observations. Extruded samples after 1 day of carbonation in Fig. 5a show the interface of two powders indicating a thick layer changing to a thin layer. The diffraction pattern indicates an amorphous structure in the thicker area again, but the MgO phase is also observed. Carbonation of the powders for 10 days revealed thicker interface areas and the ring diffraction pattern showing crystalline phases, which can be interpreted for nesquehonite, MgO and another carbonates like magnesite.

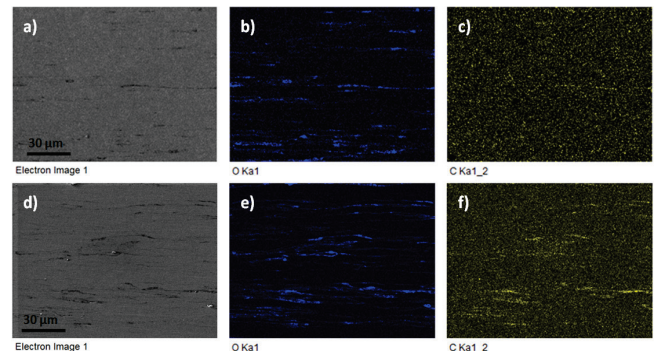


**Figure 4** Microstructure and EDX analysis of composites after extrusion: 1 day (a - c), 10 days (d - f)

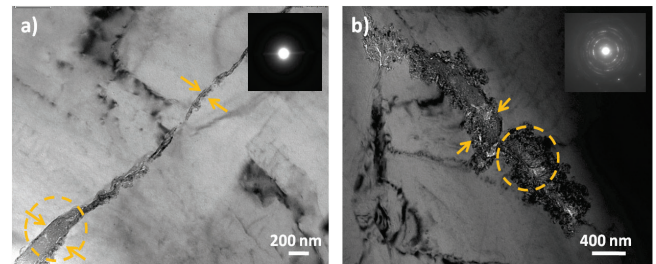


**Figure 5** TEM of the interface area: a) 1 day, b) 10 days

The tensile properties of pure and carbonated Mg samples are listed in Tab. 1. Because of the similar grain size and deformation strengthening, the extruded samples show comparable results, and the interface modification affects the mechanical properties just slightly. Without any treatment, the tensile yield strength (YS) and ultimate tensile strength (UTS) of pure Mg are 183 MPa and 268 MPa. After carbonation, the YS is slightly reduced, showing no dependency according to the number of carbonation days. However, the UTS tends to decrease with the increasing amount of carbonates on the surface.

**Table 1** Comparison of mechanical properties and corrosion rate of Mg samples

Sample	YS (MPa)	UTS (MPa)	Elongation (%)	CR (mg/cm <sup>2</sup> /day)
Pure Mg	183	268	5,8	2,12
Mg 1D	178	250	5,3	1,12
Mg 10D	176	243	5,3	3,39

YS-Yield strength, UTS-Ultimate tensile strength, CR-corrosion rate

The corrosion rate of the non-treated magnesium sample was 2,12 mg·cm<sup>-2</sup>·day<sup>-1</sup>. The mass loss obtained from the H<sub>2</sub> evolution of the carbonated sample for 1 day gave an average

corrosion rate of  $1,12 \text{ mg}\cdot\text{cm}^{-2}\cdot\text{day}^{-1}$ , which indicates a significant enhancement of corrosion properties compared to pure Mg. During the first 24 hours, the hydrogen evolution for pure Mg and Mg 1D mainly followed the same order; however, after that, the corrosion of pure magnesium was still exponential, while the corrosion rate of the carbonated sample was slowly stabilizing. Compared to previous samples, the corrosion rate of Mg 10D was considerably accelerated. Although the thicker layer of carbonates does not significantly affect the mechanical properties, the transformation from amorphous to crystalline forms significantly impacts corrosion.

#### 4 CONCLUSION

Carbonation of Mg powder native oxide surface with a simple experimental setup was studied in this work, focusing on corrosion enhancement after forward extrusion. Based on the experimental results and characterizations, the following conclusions can be reached:

The nanocrystalline native oxide (MgO) on atomized Mg powders covers the powder non-homogenously. It has a 2 layer-based interface: a dense layer (DL) and a porous layer (PL) consisting from MgO nanocrystals.

Simple carbonation of the native oxide layer can be achieved in a CO<sub>2</sub> environment. After 1 day of carbonation, the native oxide layer absorbs CO<sub>2</sub> and forms an amorphous structure. After 10 days of carbonation, the native oxide layer grows into a crystalline phase consisting mainly of nesquehonite.

Although the mechanical properties after carbonation showed no improvement over pure Mg, the conversion of native oxide into carbonates had a crucial effect on corrosion. If the formed carbonate layer is amorphous, it acts as the corrosion inhibitor, reducing the corrosion rate by half after one day of carbonation.

#### Acknowledgements

Financial support from the APVV-20-0417 and VEGA 2/0143/22 projects is gratefully acknowledged.

#### 5 REFERENCES

[1] Staiger M. P., Pietak A. M., Huadmai J. & Dias G. (2006). Magnesium and its alloys as orthopedic biomaterials: a review. *Biomaterials*, 27, 1728-1734. <https://doi.org/10.1016/j.biomaterials.2005.10.003>

[2] Witte, F., Ulrich, H., Rudert, M. & Willbold, E. (2007). Biodegradable magnesium scaffolds: Part I: appropriate inflammatory response. *Journal of Biomedical Materials Research, Part A*, 81 (7), 48-56. <https://doi.org/10.1002/jbmr.a.31170>

[3] Satya Prasad, S. V., Prasad, S. B., et al. (2022). The role and significance of Magnesium in modern day research-A review. *Journal of Magnesium and Alloys*, 10(1), 1-61. <https://doi.org/10.1016/j.jma.2021.05.012>

[4] Gardnio S., Fanetti M., Valant, M. & Orlov, D. (2016). Atomic Level Mechanism of Magnesium Oxidation. *Magnesium Technology*, 16. <https://doi.org/10.1002/9781119274803.ch16>

[5] Nie, H., Schoenitz, M. & Dreizin, E. (2016). Oxidation of Magnesium: Implication for Aging and Ignition. *Journal of Physical Chemistry C*, 120(2), 974-983. <https://doi.org/10.1021/acs.jpcc.5b08848>

[6] Bram, M., Ebel, T., Wolff, M., Cysne Barbosa, A. P. & Tuncer, N. (2013). Applications of powder metallurgy in Biomaterials. *Advances in Powder Metallurgy*, 520-554. <https://doi.org/10.1533/9780857098900.4.520>

[7] Razouk, R. I. & Mikhail, R. Sh. (1958). The Hydration of Magnesium Oxide from the Vapor Phase. *Journal of Physical Chemistry*, 62, 920-925. <https://doi.org/10.1021/j150566a006>

[8] Kato, Y., Yamashita, N., Kobayashi, K. & Yoshizawa, Y. (1996). Kinetic Study of the Hydration of Magnesium Oxide for a Chemical Heat Pump. *Applied Thermal Engineering*, 16(11), 853-862. [https://doi.org/10.1016/1359-4311\(96\)00009-9](https://doi.org/10.1016/1359-4311(96)00009-9)

[9] Taheri, M., Phillips, R. C., Kish, J. R. & Botton, G. A. (2012). Analysis of the Surface Film Formed on Mg by Exposure to Water Using a Fib Cross-Section and Stem-Eds. *Corrosion Science*, 59, 222-228. <https://doi.org/10.1016/j.corsci.2012.03.001>

[10] Taheri, M., Danaie, M. & Kisha, J. R. (2014). Tem Examination of the Film Formed on Corroding Mg Prior to Breakdown. *Journal of Electrochemical Society*, 161(3), C89-C94. <https://doi.org/10.1149/2.017403jes>

[11] Song, G. (2005). Recent Progress in Corrosion and Protection of Magnesium Alloys. *Advanced Engineering Materials*, 7(7), 563-586. <https://doi.org/10.1002/adem.200500013>

[12] Carboneras, M., Hernández, L. S., del Valle, J. A., Haría-Alonso, M. C. & Escudero, M. L. (2010). Corrosion protection of different environmentally friendly coatings on powder metallurgy magnesium. *Journal of Alloys and Compounds*, 496(1-2), 442-448. <https://doi.org/10.1016/j.jallcom.2010.02.043>

[13] Li, Y. C., Ren, Y. & Zhou, G. S. (2019). Technical note: a high corrosion-resistant Al<sub>2</sub>O<sub>3</sub>/MgO composite coating of a magnesium alloy AZ33 by chemical conversion. *Corrosion*, 75(4), 335-339. <https://doi.org/10.5006/2861>

[14] Hu, R. G., Zhang, S., Bu, J. F., Lin, C. J. & Song, G. L. (2012). Recent Progress in Corrosion and Protection of Magnesium Alloys by Organic Coatings. *Progress in Organic Coatings*, 73(2-3), 129-141. <https://doi.org/10.1016/j.porgcoat.2011.10.011>

[15] Asl, V. Z., Chini, S. F., Zhao, J. M., Palizdar, Y., Shaker, M. & Sadeghi, A. (2022). Corrosion properties and surface free energy of the Zn-Al LDH/rGO coating on MAO pretreated AZ31 magnesium alloy. *Surface and Coatings Technology*, 437, 128354. <https://doi.org/10.1016/j.surfcoat.2021.127764>

[16] Wang, Y. C., Liu, B. Y., Zhao, X. A., Zhang, X. H., Miao, Y. C., Yang, N., Yang, B., Zhang, L. Q., Kuang, W. J., Li J., Ma, E. & Shan, Z. W. (2018). Turning a native or corroded Mg alloy surface into an anti-corrosion coating in excited CO<sub>2</sub>. *Nature Communications*, 9, 4058. <https://doi.org/10.1038/s41467-018-06433-5>

[17] Xu, W. Q., Birbilis, N., Sha, G., Wang, Y., Daniels, J. E., Xiao, Y. & Ferry, M. (2015). A high-specific strength and corrosion-resistant magnesium alloy. *Nature Materials*, 14, 1229-1235. <https://doi.org/10.1038/nmat4435>

[18] Takht Ravanchi, M. & Sahebdehfar S. (2021). Catalytic conversions of CO<sub>2</sub> to help mitigate climate change: Recent process developments. *Process Safety and Environmental Protection*, 145, 172-194. <https://doi.org/10.1016/j.psep.2020.08.003>

[19] Feng, B., An, H. & Tan, E. (2007). Screening of CO<sub>2</sub> adsorbing materials for zero emission power generation system. *Energy Fuels*, 21(2), 426-434. <https://doi.org/10.1021/ef0604036>

[20] Li, Y., Kang, Z., Zhang, X., Pan, J., Ren, Y. & Zhou, G. (2022). Fabricating an anti-corrosion carbonate coating on Mg-Li alloy

by low temperature plasma. *Surface and Coatings Technology*, 439, p. 128418. <https://doi.org/10.1016/j.surfcoat.2022.128418>

- [21] Březina M., Minda J., Doležal P., Krystýnová M., Fintová S., Zapletal J., Wasserbauer J. & Ptáček P. (2017). Characterization of powder processed pure magnesium materials for biomedical applications. *Metals*, 7(11), p. 461. <https://doi.org/10.3390/met7110461>

**Authors' contacts:**

**Veronika Nagy Trembošová**

(Corresponding author)

Institute of Materials and Machine Mechanics, SAV, v. v. i.  
Dubravská cesta 9/6319, 845 13 Bratislava, Slovakia  
ummstrem@savba.sk  
veronika.trembosova@savba.sk

Slovak University of Technology in Bratislava, Faculty of Materials Science and Technology in Trnava,  
J. Bottu 25, 917 24 Trnava, Slovak Republic

**Štefan Nagy**, grades and ranks

Institute of Materials and Machine Mechanics, SAV, v. v. i.  
Dubravská cesta 9/6319, 845 13 Bratislava, Slovakia  
nagy.stefan@savba.sk

**Martin Nosko**

Institute of Materials and Machine Mechanics, SAV, v. v. i.  
Dubravská cesta 9/6319, 845 13 Bratislava, Slovakia  
martin.nosko@savba.sk

**Peter Švec**

Centre of Excellence for Advanced Materials Application, SAV, v. v. i.  
Dúbravska cesta 9, 845 11 Bratislava, Slovakia  
peter-svec@savba.sk

**Matej Štěpánek**

Institute of Materials and Machine Mechanics, SAV, v. v. i.  
Dubravská cesta 9/6319, 845 13 Bratislava, Slovakia  
matej.stepanek@savba.sk

**Otto Bajana**

Institute of Materials and Machine Mechanics, SAV, v. v. i.  
Dubravská cesta 9/6319, 845 13 Bratislava, Slovakia  
otto.bajana@savba.sk